Applied Acoustics 145 (2019) 7–24

Contents lists available at ScienceDirect

Applied Acoustics

journal homepage: www.elsevier.com/locate/apacoust

Study of sound transmission through single- and double-walled plates with absorbing material: Experimental and analytical investigation

Pouria Oliazadeh [a], Anooshiravan Farshidianfar [a,*], Malcolm J. Crocker [b]

[a] Department of Mechanical Engineering, Ferdowsi University of Mashhad, Mashhad, Iran
[b] Department of Mechanical Engineering, Auburn University, Auburn, AL 36849, United States

A R T I C L E I N F O

Article history:
Received 31 January 2018
Received in revised form 25 August 2018
Accepted 17 September 2018

Keywords:
SEA theory
Sound intensity method
Sound transmission loss
Thin rectangular plate
Transmission suite method

A B S T R A C T

In this work, the authors study sound transmission through single- and double-walled thin rectangular plates of finite extent, theoretically and experimentally. For this purpose, statistical energy analysis (SEA) is developed to predict the sound transmission loss of the plates. The essential SEA parameters, modal density and loss factors, are calculated and expressions for the sound transmission loss based on the SEA method are presented for both single- and double-walled plates. In order to validate the analytical results obtained for the transmission loss, an experimental setup was constructed including two reverberant chambers and a plate structure. The plate was placed between two rooms and the rooms were made in such a way that the sound waves propagate from the source room to the receiving room only through the rectangular panel. The sound transmission losses evaluated from the SEA models are compared with the experimental results which show good agreement. Three experimental methods were used to measure the transmission loss: The transmission suite method, a sound intensity method with a direct approach and a sound intensity method with an indirect approach. It is shown that the sound intensity method with a direct approach is more accurate than the other methods. This latter method could predict the critical frequency of the plate with only 0.5% error, whereas the other two methods had an error of more than 5%. The effects of using absorbing materials with single-walled plates were investigated experimentally and the effects of filling the cavity of double-walled plates with absorbing materials were also studied analytically. It was found that filling the cavity of the double-walled plate with lightweight absorbing material such as fiberglass increases the sound transmission loss at the critical frequency from 39 dB to a value slightly more than 53 dB. Also about 45 dB improvement in noise reduction is achieved in comparison to a similar single-walled plate.

1. Introduction

Thin rectangular plates have a wide variety of engineering applications in various industries. They are used in architectural structures, bridges, naval structures, machine parts and also aerospace structures such as tail surfaces, flaps and fins of aircraft. Extensive studies in the area of the acoustic behavior of thin plates have been carried out in the last few decades. This is mainly because achieving a suitable acoustical condition has become the main goal of designers and engineers specially in structures subjected to noise such as automotive and aircraft or in places with specific acoustical standards such as concert halls.

The control of noise is of particular importance in occupied spaces in buildings, hotels, offices and residences, where noise annoyance is caused by sound transmitted between rooms through the wall structures and from heating, ventilation and air-conditioning mechanical rooms [1,2]. Various innovative approaches have been proposed by researchers for sound attenuation and insulation of plate structures. Sound transmission loss has been used in numerous studies as a criterion for noise reduction and is defined as the ratio of the incident sound energy relative to the transmitted sound energy expressed in decibels [1]. These studies can be categorized into two groups; one based on finite plate models, whereas the other is based on infinite plate models.

Trochidis and Kalaroutis [3] studied sound transmission through double partitions. They presented a simple model of two infinite parallel thin plates containing sound absorbing materials between them. Chonan and Kugo [4] obtained an exact solution for the sound transmission loss of two-layered infinite plates based on two-dimensional elasticity theory. Steel [5] analyzed sound transmission at joints between plates in framed structures such

* Corresponding author.
E-mail address: farshid@um.ac.ir (A. Farshidianfar).

https://doi.org/10.1016/j.apacoust.2018.09.014
0003-682X/

as rooms that are constructed using partitions. Osipov, Mees and Vermeir [6] investigated the airborne sound transmission of single partitions in the low frequency range of 20 Hz – 250 Hz. Liu, Cai and Lam [7] studied sound transmission and reflection of an infinite plate immersed in fluids. They showed that attaching a coating layer of thickness 0.1 m on the incident side can decrease the sound reflection by about 6 dB above a frequency of 10 kHz. Campolina et al. [8] examined the effect of porous material lined with an isotropic plate on the sound transmission of a single-walled plate using the transfer matrix method. They also carried out several experiments to measure the transmission loss and placed a plate between a reverberant room and an anechoic room. They measured the transmitted sound power by intensimetry and deduced the incident sound power from measuring the sound pressure level and assuming a diffuse sound field inside the reverberant room. Zhou, Bhaskar and Zhang [9] optimized sound transmission through a double-walled plate by minimizing its weight and maximizing the transmission loss. All of these studies are based on infinite models and almost all of them used the wave propagation approach in order to compute the transmission loss. Pellicier and Trompette [10] published a review paper about models based on the wave approach for calculating transmission loss in infinite partitions.

The wave approach used in predicting sound transmission through infinite plates does not consider the effects of boundary conditions in theoretical calculations. An approach which is suggested for finite models of plate structures with defined boundary condition is the statistical energy analysis (SEA) method. The SEA method was developed by Maidanik [11], Lyon [12] and Crocker and Price [13]. In the SEA method, a system is modeled as several subsystems. Each subsystem may receive input power by an external source. The input powers flow from one subsystem to other subsystems and can be dissipated because of the damping in each subsystem. Therefore, the effect of dissipation in sound transmission can also be taken into account in the SEA method.

Jean and Roland [14] presented a simple SEA method to predict the sound insulation between dwellings. Hynna, Klinge and Vuoksinen [15] used the SEA method for predictions of structure-borne sound transmission in large welded ship structures. Craik, Steel and Evans [16] also studied the influence of resonant modes in the low frequency range while using the SEA method for structure-borne sound transmission. Osipov and Vermeir [17] investigated the effect of elastic layers at junctions on airborne and structure-borne sound transmission in buildings. Hopkins [18] presented measured data for the validation of SEA evaluations of sound transmission through masonry cavity wall constructions. Craik and Smith [19,20] investigated airborne and structure-borne sound transmission through double leaf lightweight partitions. They examined different SEA models based on the details of construction and categorized them as SEA models of a double wall with no structural connections, with structural coupling at a few point connections and with structural coupling as a line connection. They found out that the performance of each model is dependent on the frequency range and the construction details. In this paper, no structural coupling is assumed for the double-walled plate. Therefore, the first SEA model was used. Zhou and Crocker [21] analyzed sound transmission through honeycomb sandwich panels. They developed a closed form solution for the modal density of sandwich plates which is one of the important and essential parameters that is involved in the SEA modeling. Reynders et al. [22] presented a stochastic method, consisting of finite element method (FEM) and SEA method. They showed that this hybrid approach is suited for the mid-frequency analysis of sound transmission through a wall between two rooms. Although the FEM approach is useful for predicting the sound transmission between rooms in the low- and mid-frequency range, it becomes unmanageable at high frequencies, in which the number of finite elements becomes very large. However, it can be used in estimating the modal density and other modal parameters needed in plate and cylindrical shell structures [23,24].

Besides the wave approach and the SEA method, other methods such as transfer matrix methods [25] and FEM numerical methods [26] have also been used in order to investigate the sound transmission through plate structures.

Experimental techniques have also been developed to measure the sound transmission loss of structures. Wang, Crocker and Raju [27] measured the transmission loss of an aluminum cylinder using the sound intensity technique and the transmission suite method. Chen et al. [28] used the sound intensity method in order to measure damping components of plates. Connelly and Hodgson [29] studied the sound transmission of vegetated roofs experimentally using the sound intensity method. Oliazadeh, Farshidianfar and Crocker [30] recently studied the sound transmission through a cylindrical shell with absorbing material using both the transmission suite and sound intensity methods. They compared the experimental results with those obtained by the SEA theory. Luo, Sun and Wen studied the influence of the boundary conditions on the modal parameters of thin cylindrical shell [31]. Composite cylindrical shells are being increasingly used as aircraft cabins instead of metal ones. Florence, Renji and Subramanian have now extended studies on cylindrical shells to those made of honeycomb sandwich composite [32].

In the present work, a finite model for sound transmission through a panel is considered. Therefore, the SEA theory is used in order to find the sound transmission loss of a thin single-walled rectangular plate and the theory is developed for a double-walled plate. The analytical expression is obtained and presented for each of the single- and double-walled plates. The transmission loss is also measured using three experimental methods, the transmission suite method, the sound intensity method with a direct approach and the sound intensity method with an indirect approach. The effectiveness of each method is discussed by comparing the analytical and experimental results. Then the effects of applying absorbing material in the design of single- and double-walled plate structures are examined completely.

2. Theoretical Model

Consider a rectangular plate with length l_x and width l_y in the x and y directions, respectively and thickness $h \ll l_x$ and l_y lying in the $x-y$ plane, as shown in Fig. 1. The plate material is assumed to be isotropic, homogeneous and elastic with Poisson ratio ν, *in vacuo* bulk mass density ρ, and *in vacuo* Young's modulus of elasticity E. It is assumed that the plate has uniform thickness and undergoes small displacements. The partial differential equation of motion of a plate can be obtained by employing equilibrium equations of forces and moments for a section of the plate and using Hooke's law to find their constitutive elations [33].

$$D\left(\frac{\partial^4 w}{\partial x^4} + 2\frac{\partial^4 w}{\partial x^2 \partial y^2} + \frac{\partial^4 w}{\partial y^4}\right) + \rho h \frac{\partial^2 w}{\partial t^2} = 0, \tag{1}$$

where $w(x, y, t)$ is the transverse displacement of the neutral plane of the plate and D is the flexural rigidity of the plate which is defined by

$$D = \frac{Eh^3}{12(1-\nu^2)}. \tag{2}$$

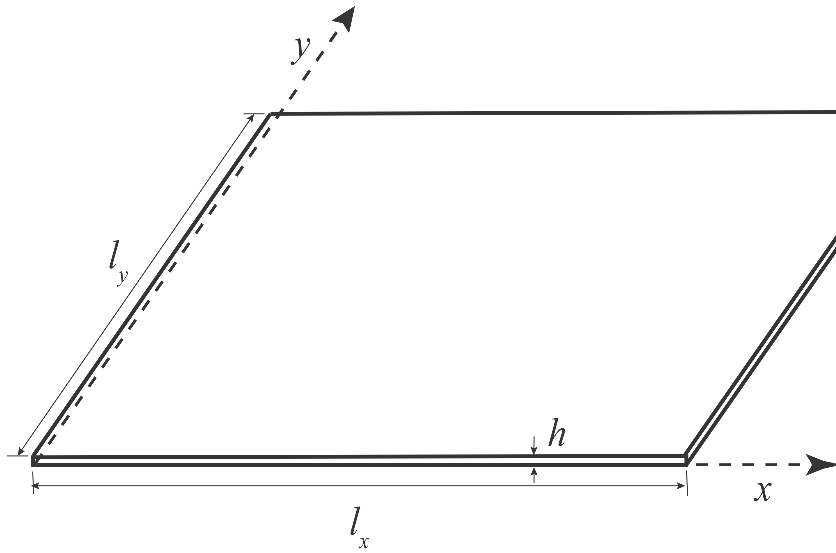

Fig. 1. Thin rectangular plate.

2.1. Natural frequency of a clamped plate

The expression for calculating the natural frequencies of a clamped thin rectangular plate can be obtained using the Rayleigh-Ritz method. Therefore, the angular natural frequency, ω_{mn}, is given by [33]

$$\omega_{mn} = \left(\frac{\pi}{l_x}\right)^2 \sqrt{\frac{D}{\rho h}\left[\Phi_m^4 + \Phi_n^4\left(\frac{l_x}{l_y}\right)^4 + 2\left(\frac{l_x}{l_y}\right)^2\right](\Psi_m \Psi_n)}, \tag{3}$$

where m and n are the mode numbers along the x and y directions, respectively and

$$\Phi_m = \begin{cases} 1.506 & m = 2 \\ m - 0.5 & m > 2 \end{cases}, \tag{4a}$$

$$\Phi_n = \begin{cases} 1.506 & n = 2 \\ n - 0.5 & n > 2 \end{cases}, \tag{4b}$$

$$\Psi_m = \begin{cases} 1.248 & m = 2 \\ (m - 0.5)^2\left[1 - \frac{2}{\pi(m-0.5)}\right] & m > 2 \end{cases}, \tag{4c}$$

$$\Psi_n = \begin{cases} 1.248 & n = 2 \\ (n - 0.5)^2\left[1 - \frac{2}{\pi(n-0.5)}\right] & n > 2 \end{cases}. \tag{4d}$$

The Rayleigh-Ritz method is described in detail in the references mentioned in the literature. However, the details of obtaining the mode shape of vibration of a clamped plate is explained in the Appendix.

2.2. SEA model

In the statistical energy analysis (SEA) method, the structures under investigation are divided into a number of subsystems. The behavior of each subsystem is related to its modal energy and the response of the entire model can be characterized by predicting the coupling between subsystems. The power flow between subsystems comes from the input energy of each subsystem which is assumed to be due to random external sources. This amount of energy that enters the system is transferred from one subsystem to others and some part of it is dissipated by mechanical damping in the subsystems.

Consider that the thin rectangular panel is clamped between two reverberant rooms and is excited by a loudspeaker in one of the rooms which is called the source room or transmission room. The other room, in which the transmitted sound propagates is called the receiving room or reception room. Using the procedure presented in Refs. [13,34], SEA models are developed here by considering the effect of non-resonant power flow between the source room and the receiving room in double-walled systems. The influence of using absorbing material in both the single- and double-walled systems is also considered. Therefore, new equations are obtained for the SEA modeling of single- and double-walled plates which are explained in detail in this section.

The SEA models for single- and double-walled plates which consist of three and five coupled subsystems, respectively are shown schematically in Fig. 2, see [13,34]. In the first SEA model, the source room and the receiving room are considered as subsystems 1 and 3, respectively and the panel structure is assumed as subsystem 2 [13]. In the second SEA model, the source and receiving rooms are considered as subsystems 1 and 5, respectively, the first and second walls of the plate are considered as subsystems 2 and 4, respectively and the cavity between the plate walls is assumed to be subsystem 3 [34]. The SEA matrix for models 1 and 2 is given in Eqs. (5) and (6), respectively considering that the exchange of energy is proportional to the modal energy difference [12].

$$\omega \begin{bmatrix} \eta_1 & -\eta_{21} & -\eta_{31} \\ -\eta_{12} & \eta_2 & -\eta_{32} \\ -\eta_{13} & -\eta_{23} & \eta_3 \end{bmatrix} \begin{Bmatrix} E_1 \\ E_2 \\ E_3 \end{Bmatrix} = \begin{Bmatrix} \Pi_1 \\ \Pi_2 \\ \Pi_3 \end{Bmatrix} \tag{5}$$

$$\omega \begin{bmatrix} \eta_1 & -\eta_{21} & -\eta_{31} & 0 & -\eta_{51} \\ -\eta_{12} & \eta_2 & -\eta_{32} & 0 & 0 \\ -\eta_{13} & -\eta_{23} & \eta_3 & -\eta_{43} & -\eta_{53} \\ 0 & 0 & -\eta_{34} & \eta_4 & -\eta_{54} \\ -\eta_{15} & 0 & -\eta_{35} & -\eta_{45} & -\eta_5 \end{bmatrix} \begin{Bmatrix} E_1 \\ E_2 \\ E_3 \\ E_4 \\ E_5 \end{Bmatrix} = \begin{Bmatrix} \Pi_1 \\ \Pi_2 \\ \Pi_3 \\ \Pi_4 \\ \Pi_5 \end{Bmatrix} \tag{6}$$

where $\omega = 2\pi f$ is the circular frequency of the band of interest, η_i is the internal loss factor of subsystem i, η_{ij} is the coupling loss factor between subsystems i and j, E_i is the total energy stored in subsystem i and Π_i is the rate of energy flow into subsystem i. Since the sound source is only located in the transmission room (subsystem 1), therefore the energy flow into subsystems 2, 3, 4 and 5 is zero;

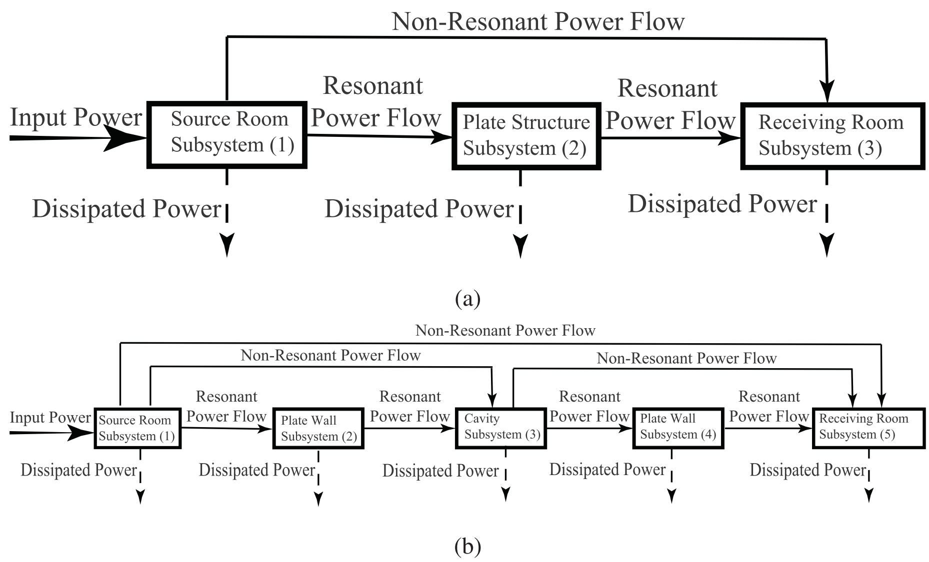

Fig. 2. Schematic display of the SEA model: (a) Single-walled plate (Model 1); (b) Double-walled plate (Model 2).

$\Pi_2 = \Pi_3 = \Pi_4 = \Pi_5 = 0$. Thus the power balance equations written in the matrix form in Eqs. (5) and (6) can be rewritten as:

$$\begin{bmatrix} \eta_1 & -\eta_{21} & -\eta_{31} \\ -\eta_{12} & \eta_2 & -\eta_{32} \\ -\eta_{13} & -\eta_{23} & \eta_3 \end{bmatrix} \begin{Bmatrix} E_1 \\ E_2 \\ E_3 \end{Bmatrix} = \begin{Bmatrix} \frac{\Pi_1}{\omega} \\ 0 \\ 0 \end{Bmatrix} \tag{7}$$

$$\begin{bmatrix} \eta_1 & -\eta_{21} & -\eta_{31} & 0 & -\eta_{51} \\ -\eta_{12} & \eta_2 & -\eta_{32} & 0 & 0 \\ -\eta_{13} & -\eta_{23} & \eta_3 & -\eta_{43} & -\eta_{53} \\ 0 & 0 & -\eta_{34} & \eta_4 & -\eta_{54} \\ -\eta_{15} & 0 & -\eta_{35} & -\eta_{45} & -\eta_5 \end{bmatrix} \begin{Bmatrix} E_1 \\ E_2 \\ E_3 \\ E_4 \\ E_5 \end{Bmatrix} = \begin{Bmatrix} \frac{\Pi_1}{\omega} \\ 0 \\ 0 \\ 0 \\ 0 \end{Bmatrix} \tag{8}$$

The energies in each subsystem are obtained by inverting the coefficient matrix of Eqs. (7) and (8). In the context of noise reduction, the energy level difference between source room and receiving room should be calculated. Hence, the ratio of total energies in these two reverberant rooms is obtained as follows for single- and double-walled plates, respectively [13,34].

$$\frac{E_3}{E_1} = \frac{\eta_{12}\eta_{23} + \eta_2\eta_{13}}{\eta_2\eta_3 - \eta_{23}\eta_{32}}, \tag{9}$$

$$\frac{E_5}{E_1} = \frac{C_1}{C_2}, \tag{10}$$

where

$$\begin{aligned} C_1 =& \eta_{13}\eta_{34}(\eta_2\eta_4 + \eta_{12}\eta_{45}) + \eta_{23}\eta_{12}(\eta_4\eta_{35} + \eta_{34}\eta_{45}) \\ &+ \eta_{15}(\eta_2\eta_3\eta_4 - \eta_4\eta_{23}\eta_{32} - \eta_2\eta_{34}\eta_{43}), \\ C_2 =& \eta_4\eta_5(\eta_{23}\eta_{32} - \eta_2\eta_3) - \eta_2\eta_{35}(\eta_{43}\eta_{54} + \eta_4\eta_{53}) \\ &+ \eta_2\eta_{34}(\eta_5\eta_{43} - \eta_{45}\eta_{53}) + \eta_{45}\eta_{54}(\eta_{23}\eta_{32} - \eta_2\eta_3). \end{aligned} \tag{11}$$

The noise reduction is then evaluated by taking the logarithm of Eqs. (9) and (10). The coupling loss factors in the reverse direction are calculated using the reciprocity relationship [12].

$$\eta_{ij}n_i = \eta_{ji}n_j \tag{12}$$

where n_i and n_j are the modal densities of subsystems i and j, respectively. Therefore Eqs. (9) and (10) become

$$\frac{E_3}{E_1} = \frac{(\frac{n_2}{n_1})\eta_{21}\eta_{23} + \eta_2\eta_{13}}{\eta_2\eta_3 - \frac{n_2}{n_3}\eta_{23}^2}, \tag{13}$$

$$\frac{E_5}{E_1} = \frac{C_3}{C_4}, \tag{14}$$

where

$$\begin{aligned} C_3 =& \left(\frac{n_4}{n_1}\right)\eta_{31}\eta_{43}\left[\eta_2\eta_4 + \left(\frac{n_2}{n_1}\right)\eta_{21}\eta_{45}\right] + \left(\frac{n_2}{n_1}\right)\eta_{21}\eta_{23}\left[\eta_4\eta_{35} + \left(\frac{n_4}{n_3}\right)\eta_{43}\eta_{45}\right] \\ &+ \eta_{15}\left[\eta_2\eta_3\eta_4 - \left(\frac{n_2}{n_3}\right)\eta_4\eta_{23}^2 - \left(\frac{n_4}{n_3}\right)\eta_2\eta_{43}^2\right], \\ C_4 =& \eta_4\eta_5\left[\left(\frac{n_2}{n_3}\right)\eta_{23}^2 - \eta_2\eta_3\right] - \eta_2\eta_{35}\left[\left(\frac{n_4}{n_5}\right)\eta_{43}\eta_{45} + \left(\frac{n_3}{n_5}\right)\eta_4\eta_{35}\right] \\ &+ \left(\frac{n_4}{n_3}\right)\eta_2\eta_{43}\left[\eta_5\eta_{43} - \left(\frac{n_3}{n_5}\right)\eta_{45}\eta_{35}\right] + \left(\frac{n_4}{n_5}\right)\eta_{45}^2\left[\left(\frac{n_2}{n_3}\right)\eta_{23}^2 - \eta_2\eta_3\right]. \end{aligned} \tag{15}$$

In order to obtain the noise reduction, the parameters of Eqs. (13) and (14) must be calculated first.

2.3. Modal density

n_1, n_2 and n_3 in Eq. (13) are the statistical modal densities of the source room, the thin rectangular plate and the receiving room, respectively. While n_1, n_2, n_3, n_4 and n_5 in Eq. (14) are the statistical modal densities of the source room, first wall of the plate, cavity, second wall of the plate and the receiving room, respectively. The modal densities of the acoustical spaces (source room and receiving room) are given by [12]

$$n_i(f) = \frac{4\pi f^2 V_i}{c_{\text{air}}^3} + \frac{\pi f S_i}{2c_{\text{air}}^2} + \frac{P_i}{8c_{\text{air}}}, \quad i = \begin{cases} 1 \text{ and } 3 & \text{single-walled plate} \\ 1 \text{ and } 5 & \text{double-walled plate} \end{cases} \tag{16}$$

where V_i is the volume of the acoustical element, S_i is the total surface area of the acoustical element, P_i is the total edge length of the acoustical element and c_{air} is the speed of sound in air. The modal density of the cavity in the double-walled plate model is expressed as [19]

$$n_i(f) = \frac{2\pi f S_i}{c_{\text{air}}^2}, \quad i = 3 \quad \text{double-walled plate} \tag{17}$$

The modal density of the thin panel is defined as the number of natural frequencies per hertz and is given by [35]

$$n_i(f) = \frac{\sqrt{3}S_i}{c_{\text{plate}}h}, \quad i = \begin{cases} 2 & \text{single-walled plate} \\ 2 \text{ and } 4 & \text{double-walled plate} \end{cases} \tag{18}$$

where S_i is the surface area of the plate and c_{plate} is the speed of quasi-longitudinal waves in the plate which is obtained from [35]

$$c_{plate} = \sqrt{\frac{E}{\rho(1-\nu^2)}}. \tag{19}$$

The modal density can also be expressed as the number of natural frequencies per radian per second, $n_i(\omega)$, which is $1/(2\pi)$ times $n_i(f)$.

$$n_i(\omega) = \frac{\sqrt{3}S_i}{2\pi c_{plate} h}, \quad i = \begin{cases} 2 & \text{single-walled plate} \\ 2 \text{ and } 4 & \text{double-walled plate} \end{cases} \tag{20}$$

2.4. Loss factor

The loss factors in Eqs. (13) and (14) include internal loss factors of the plate, cavity and receiving room, coupling loss factors between the acoustical spaces (reverberant rooms and cavity) and the coupling loss factors due to sound radiation from the plate to the acoustical spaces (reverberant rooms and cavity).

The internal loss factor of the lightly damped plate can be assumed to vary from 0.001 to 0.05 [35]. Furthermore, since the dissipation mechanism is caused by radiation damping, the following expression can be used [15]

$$\eta_i = 0.041 f^{-0.7}, \quad i = \begin{cases} 2 & \text{single-walled plate} \\ 2 \text{ and } 4 & \text{double-walled plate} \end{cases}. \tag{21}$$

The internal loss factor of the receiving room is obtained from [36]

$$\eta_i = \frac{2.2}{f T_{60}}, \quad i = \begin{cases} 3 & \text{single-walled plate} \\ 5 & \text{double-walled plate} \end{cases}, \tag{22}$$

where T_{60} is the reverberation time of the acoustical space that can be measured experimentally or calculated analytically using the following equation [1,37]

$$T_{60} = \frac{55.26 V_i}{c_{air} S_i}, \quad i = \begin{cases} 3 & \text{single-walled plate} \\ 5 & \text{double-walled plate} \end{cases}. \tag{23}$$

The internal loss factor of the cavity in a double-walled system is assumed to be $\eta_3 < 0.1$ for the case that it is not lined with absorbing material. The coupling loss factor between source and receiving spaces for the single- and double-walled plates is obtained from Eqs. (24) and (25), respectively [38]

$$\eta_{13} = \frac{c_{air} S_2}{8\pi f V_1} \tau_{13}, \tag{24}$$

$$\eta_{15} = \frac{c_{air} S_2}{8\pi f V_1} \tau_{15}, \tag{25}$$

in which τ_{13} and τ_{15} are the mass law transmission coefficients due to non-resonant transmission from the source room to the receiving room. τ_{13} and τ_{15} for normally incident sound are defined by [26]

$$\tau_{13}^{normal} = \frac{1}{1 + \left(\frac{\pi f \rho h}{\rho_{air} c_{air}}\right)^2}, \tag{26a}$$

$$\tau_{15}^{normal} = \frac{1}{1 + \left[\frac{\pi f (2\rho h + \rho_{air} d)}{\rho_{air} c_{air}}\right]^2}, \tag{26b}$$

where ρ_{air} is the mass density of air and d is the distance between the plate walls.

The mass law transmission coefficient for a normal plane wave does not provide an appropriate physical interpretation for the sound transmission mechanism. The effect of incidence angle should be taken into account in order to gain a physical insight which conforms to reality. Therefore, the mass law transmission coefficient for spherical wave incidence or diffuse incidence is suggested. τ_{13} and τ_{15} for the spherical wave incidence [39] and the diffuse incidence [40] are defined by the following equations:

$$\tau_{13}^{spherical} = \frac{\tan^{-1}\left(\frac{\pi f \rho h}{\rho_{air} c_{air}}\right)}{\frac{\pi f \rho h}{\rho_{air} c_{air}}}, \tag{27a}$$

$$\tau_{15}^{spherical} = \frac{\tan^{-1}\left[\frac{\pi f (2\rho h + \rho_{air} d)}{\rho_{air} c_{air}}\right]}{\frac{\pi f (2\rho h + \rho_{air} d)}{\rho_{air} c_{air}}}, \tag{27b}$$

$$\tau_{13}^{diffuse} = \frac{\ln\left[1 + \left(\frac{\pi f \rho h}{\rho_{air} c_{air}}\right)^2\right]}{\left(\frac{\pi f \rho h}{\rho_{air} c_{air}}\right)^2}, \tag{28a}$$

$$\tau_{15}^{diffuse} = \frac{\ln\left[1 + \left[\frac{\pi f (2\rho h + \rho_{air} d)}{\rho_{air} c_{air}}\right]^2\right]}{\left[\frac{\pi f (2\rho h + \rho_{air} d)}{\rho_{air} c_{air}}\right]^2}. \tag{28b}$$

The coupling loss factors between the cavity, which is assumed as a two-dimensional sound field, and the source and receiving rooms for non-resonant transmission in the double-walled plate model are given by [41]

$$\eta_{31} = \eta_{35} = \frac{\rho_{air}^2 c_{air}^3 S_2 \sigma_{f_{critical}}}{8\pi^3 f^3 (\rho h)^2 V_3}, \tag{29}$$

where $\sigma_{f_{critical}}$ is the radiation efficiency of the plate at its critical frequency. The radiation efficiency is explained in detail in the next section.

In addition to the loss factors calculated so far, the SEA models also require the coupling between the thin plate and both reverberant rooms and cavity. The coupling loss factors from the structure to the acoustical media in the single- and double-walled plate models are given by Eqs. (30) and (31), respectively [42]

$$\eta_{21} = \eta_{23} = \frac{\rho_{air} c_{air} \sigma}{2\pi f \rho h}, \tag{30}$$

$$\eta_{21} = \eta_{23} = \eta_{43} = \eta_{45} = \frac{\rho_{air} c_{air} \sigma}{2\pi f \rho h}, \tag{31}$$

where σ is the radiation efficiency of the plate.

2.5. Radiation efficiency

The radiation efficiency of a structural element such as a plate is derived from the radiated acoustic intensity, I [6] or the radiated sound power, P [14] and the mean quadratic surface velocity, $< v^2 >$ using the following equations.

$$\sigma = \frac{I}{\rho_{air} c_{air} < v^2 >}, \tag{32a}$$

$$\sigma = \frac{P}{\rho_{air} c_{air} S_2 < v^2 >}. \tag{32b}$$

The radiation efficiency of the plate varies according to the frequency band of interest as follows:

1) For a band that includes frequencies below the plate critical frequency, the radiation efficiency is divided into the radiation efficiency in the edge mode region, σ_{edge}, and the corner mode region, σ_{corner}. The critical frequency of an isotropic plate is defined as the frequency at which the speed of bending waves in the plate is equal to the speed of sound waves in air and is given by [43]

$$f_{critical} = \frac{c_{air}^2}{2\pi h} \sqrt{\frac{12\rho(1-\nu^2)}{E}}. \tag{33}$$

Since sound transmits easily through a plate at its critical frequency, it is important to evaluate it accurately from an acoustical point of view. The σ_{corner} and σ_{edge} are expressed as [13]

$$\sigma_{\text{corner}} = \frac{8}{\pi^4}\left(\frac{\lambda^2_{\text{critical}}}{S_2}\right)\left(\frac{f}{f_{\text{critical}}}\right)\frac{1-2\left(\frac{f}{f_{\text{critical}}}\right)}{\sqrt{\frac{f}{f_{\text{critical}}}\left(1-\frac{f}{f_{\text{critical}}}\right)}}, \quad f < \frac{1}{2}f_{\text{critical}}, \tag{34a}$$

$$\sigma_{\text{edge}} = \frac{1}{4\pi^2}\left(\frac{P_2\lambda^2_{\text{critical}}}{S_2}\right)\frac{\left(1-\frac{f}{f_{\text{critical}}}\right)\ln\left[\frac{1+\sqrt{\frac{f}{f_{\text{critical}}}}}{1-\sqrt{\frac{f}{f_{\text{critical}}}}}\right]+2\sqrt{\frac{f}{f_{\text{critical}}}}}{\left(1-\frac{f}{f_{\text{critical}}}\right)\sqrt{1-\frac{f}{f_{\text{critical}}}}}, \tag{34b}$$

where $\lambda_{\text{critical}}$ is the acoustic wavelength at the critical frequency and is defined by

$$\lambda_{\text{critical}} = \frac{c_{\text{plate}}}{f_{\text{critical}}} = \frac{\pi h E}{\sqrt{3}\rho c^2_{\text{air}}(1-\nu^2)}. \tag{35}$$

In the corner mode region, the radiation efficiency is assumed to be zero for frequencies greater than $0.5f_{\text{critical}}$ and less than f_{critical}.

Oppenheimer and Dubowsky [44] introduced three correction factors for the radiation efficiency of plates below the critical frequency that account for the effect of inertial flows in the vicinity of the plate perimeter at low frequencies (ϵ_{plate}) and from corner (ϵ_{corner}) and edge (ϵ_{edge}) modes at higher frequencies. These correction factors are as follows:

$$\epsilon_{\text{plate}} = \frac{53\left(\frac{f^4S_2^2}{c^4_{\text{air}}}\right)}{1+53\left(\frac{f^4S_2^2}{c^4_{\text{air}}}\right)}, \tag{36a}$$

$$\epsilon_{\text{corner}} = \frac{13\left(\frac{f}{f_{\text{critical}}}\right)}{2\left[1+13\left(\frac{f}{f_{\text{critical}}}\right)\right]}, \tag{36b}$$

$$\epsilon_{\text{edge}} = \frac{49\left(\frac{f}{f_{\text{critical}}}\right)}{2\left[1+49\left(\frac{f}{f_{\text{critical}}}\right)\right]}. \tag{36c}$$

Hence, the total radiation efficiency can be given as:

$$\sigma = \epsilon_{\text{plate}}(\epsilon_{\text{corner}}\sigma_{\text{corner}} + \epsilon_{\text{edge}}\sigma_{\text{edge}}), \quad f < f_{\text{critical}}. \tag{37}$$

2) For frequencies around the critical frequency of a plate, the radiation efficiency is obtained as [45]

$$\sigma = \left(0.5 - \frac{0.15 l_y}{l_x}\right)\sqrt{\frac{2\pi l_y f_{\text{critical}}}{c_{\text{air}}}}, \quad f = f_{\text{critical}}. \tag{38}$$

It should be noted that l_y is assumed to be the smaller dimension of the rectangular plate in Eq. (38).

3) For a band that has frequencies above the critical frequency of a plate, the radiation efficiency is calculated using following expression [34]

$$\sigma = \frac{1}{\sqrt{1-\frac{f_{\text{critical}}}{f}}}, \quad f > f_{\text{critical}}. \tag{39}$$

2.6. Sound transmission loss

Sound transmission through a plate structure in the reverberant field causes a drop in the noise level which is called noise reduction (NR). The noise reduction can be obtained experimentally by measuring the sound pressure level in the source room and the receiving room and calculating the difference between them.

$$\text{NR} = L_{p_1} - L_{p_i}, \quad i = \begin{cases} 3 & \text{single-walled plate} \\ 5 & \text{double-walled plate} \end{cases} \tag{40}$$

where L_{p_1} is the sound pressure level in the source room and L_{p_3} and L_{p_5} are the sound pressure levels in the receiving room for the single- and double-walled plate models, respectively. The noise reduction is evaluated theoretically by taking the logarithm of Eqs. (13) and (14) for the first (NR_1) and second (NR_2) SEA models, respectively.

$$\text{NR}_1 = 10\log\left[\left(\frac{n_2}{n_1}\right)\eta_{21}\eta_{23} + \eta_2\eta_{13}\right] - 10\log\left[\eta_2\eta_3 - \left(\frac{n_2}{n_3}\right)\eta_{23}^2\right] \tag{41}$$

$$\begin{aligned}\text{NR}_2 = {} & 10\log\left[\left(\frac{n_4}{n_1}\right)\eta_{31}\eta_{43}\left[\eta_2\eta_4 + (\frac{n_2}{n_1})\eta_{21}\eta_{45}\right] + \left(\frac{n_2}{n_1}\right)\eta_{21}\eta_{23}\left[\eta_4\eta_{35} + (\frac{n_4}{n_3})\eta_{43}\eta_{45}\right]\right.\\ & \left. +\eta_{15}\left[\eta_2\eta_3\eta_4 - \left(\frac{n_2}{n_3}\right)\eta_4\eta_{23}^2 - \left(\frac{n_4}{n_3}\right)\eta_2\eta_{43}^2\right]\right] - 10\log\left[\eta_4\eta_5\left[\left(\frac{n_2}{n_3}\right)\eta_{23}^2 - \eta_2\eta_3\right]\right.\\ & -\eta_2\eta_{35}\left[\left(\frac{n_4}{n_5}\right)\eta_{43}\eta_{45} + \left(\frac{n_3}{n_5}\right)\eta_4\eta_{35}\right] + \left(\frac{n_4}{n_3}\right)\eta_2\eta_{43}\left[\eta_5\eta_{43} - \left(\frac{n_3}{n_5}\right)\eta_{45}\eta_{35}\right]\\ & \left. +\left(\frac{n_4}{n_5}\right)\eta_{45}^2\left[\left(\frac{n_2}{n_3}\right)\eta_{23}^2 - \eta_2\eta_3\right]\right]\end{aligned} \tag{42}$$

Another parameter which is usually used in the room acoustic measurements is sound transmission loss (TL). Unlike noise reduction which is influenced by the panel and the absorption in the receiving room, the transmission loss is only related to the vibrational properties of the panel (mass, damping and stiffness). Therefore, in order to investigate the acoustic behavior of a plate structure, it is more appropriate to study the transmission loss which is defined as the ratio of the incident sound power (P_{incident}) to the transmitted sound power ($P_{\text{transmitted}}$).

$$\text{TL} = 10\log\frac{P_{\text{incident}}}{P_{\text{transmitted}}} \tag{43}$$

The transmission loss is also obtained from the noise reduction by using Eqs. (44) and (45) for first (TL_1) and second (TL_2) SEA models, respectively [46]

$$\text{TL}_1 = \text{NR}_1 + 10\log\frac{S_2}{S_3} \tag{44}$$

$$\text{TL}_2 = \text{NR}_2 + 10\log\frac{2S_2 + S_3}{S_5} \tag{45}$$

3. Experimental analysis

A thin rectangular plate was constructed which was made of galvanized steel with material properties; $E = 200$ GPa, $\rho = 7850$ kg/m^3 and $\nu = 0.28$. It had length and width of 1.04 m and 0.609 m, respectively with the wall thickness of 1.27 mm. The experimental setup is shown in Fig. 3. The plate was clamped between heavy steel frames using two sets of bolts which were tightened and placed along all four edges of the frame in order to achieve clamped boundary conditions.

3.1. Analytical and experimental comparison of the natural frequency

In order to find the natural frequencies of the thin rectangular plate, two different methods of excitation were used: (1) the contact excitation method which utilized a modal hammer to excite natural frequencies of the plate and (2) the non-contact excitation

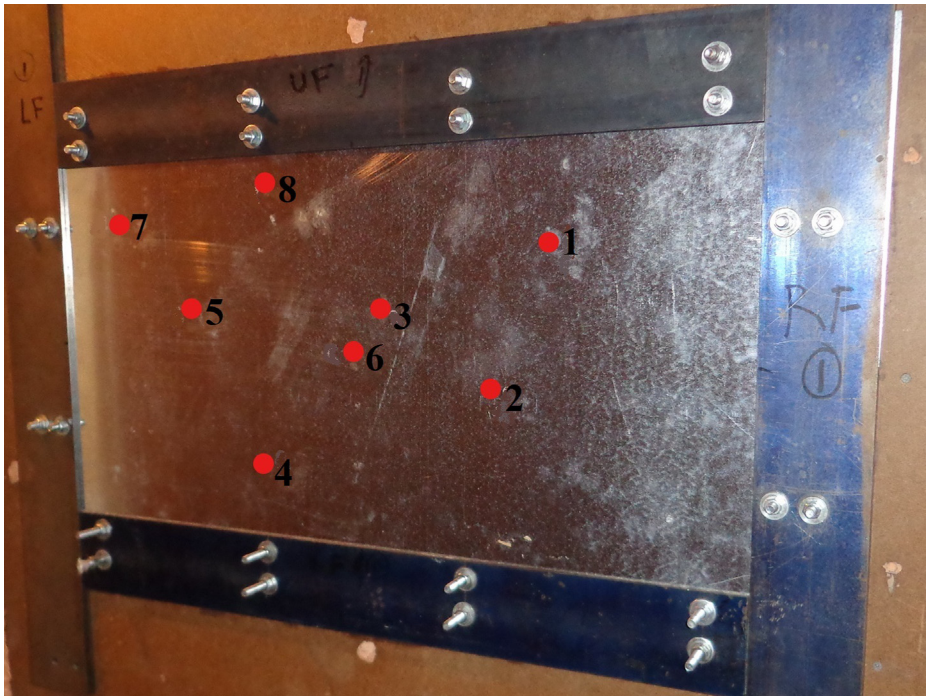

Fig. 3. Experimental setup of the thin rectangular plate.

method in which a loudspeaker was used to acoustically excite resonance frequencies of the panel.

3.1.1. Hammer excitation

Two contact excitation methods have been used by researchers for vibration analysis of thin-walled structures such as plates and cylindrical shells. These two methods are hammer and shaker excitation techniques. Using hammer allows the plate to undergo free vibration in its natural modes, because there are no external forces after the impact is applied. Therefore, this type of excitation, the hammer excitation method, was found suitable here to find natural frequencies of the plate under consideration.

Several points were chosen in order to attach the Bruel and Kjaer accelerometer (type 4375) to the surface of the panel. These points were marked on the surface of the plate from 1 to 8 as are seen in Fig. 3. The accelerometer in conjunction with a transducer was connected to a Bruel and Kjaer charge amplifier (type 2647B). The measurements were analyzed with a Bruel and Kjaer Pulse multi-analyzer system (type 3560) using the Pulse software 10.1. Several tests were carried out for various positions of the accelerometer. Fig. 4 shows the Fast Fourier Transforms (FFTs) obtained from four locations of the accelerometer. The locations of 1, 6, 7 and 8 cover all the surface of the plate including points near the boundaries, far from the boundaries, and at the middle of the plate. It was observed in the frequency range $0-1000$ Hz that the hammer excited some modes better than other modes and some of them were completely missed or barely recognizable due to their small peaks specially after 700 Hz since no noticeable peak can found in FFT graphs. There are some minor peaks at frequencies between 300 Hz and 700 Hz and most specific peaks appeared at frequencies less than 300 Hz.

3.1.2. Acoustical excitation

Three loudspeakers (Community M4, EM282 and VHF100) with different crossover frequencies were utilized in order to excite the plate through emitting a random white noise signal generated by the Bruel and Kjaer pulse system. These loudspeakers covered the low range of frequency $(200-2000$ Hz), the medium range of frequency $(1000-12000$ Hz) and the high range of frequency $(1800-18000$ Hz). The modal experiment using acoustical excitation was conducted in a reverberant chamber which is shown in Fig. 5 where the sound pressure is similar for all surface points. The Fast Fourier Transforms obtained by the acoustical excitation method for different positions of accelerometer on the surface of the panel are shown in Fig. 6. It was observed that sound waves easily excited frequencies higher than 500 Hz. This type of excitation, unlike the hammer excitation method which was efficient in the low frequency range less than 300 Hz, was more efficacious in the medium range of frequency between 500 Hz and 2000 Hz and to some extent in high frequency ranges.

The values of the first ten natural frequencies of the thin rectangular plate obtained by two experimental techniques are presented in Table 1 and compared with the theoretical results. The comparison shows very good agreement between analytical and experimental results.

3.2. The reverberation time measurement

It is necessary to find the reverberation time of the receiving room, since the internal loss factor of the receiving room is related to its reverberation time. An analytical expression was presented in the former part in order to calculate the reverberation time of a room; however, the reverberation time of the receiving room was also measured during the experiment. The Bruel and Kjaer pulse system was used for the measurement of the reverberation time. Two Pioneer loudspeakers (type CS-G405Q) were placed at opposite corners in the receiving room and were connected to the Pulse system in order to generate the sufficient noise inside the room. The Pulse software was used to evaluate the reverberation time by measuring the time needed for the sound pressure level to drop by 60 dB after switching off the sound source. Therefore, a Bruel and Kjaer microphone (type 4188L1) was also located in the receiving room to measure the sound pressure level. Fig. 7 shows the setup prepared for measuring the reverberation time

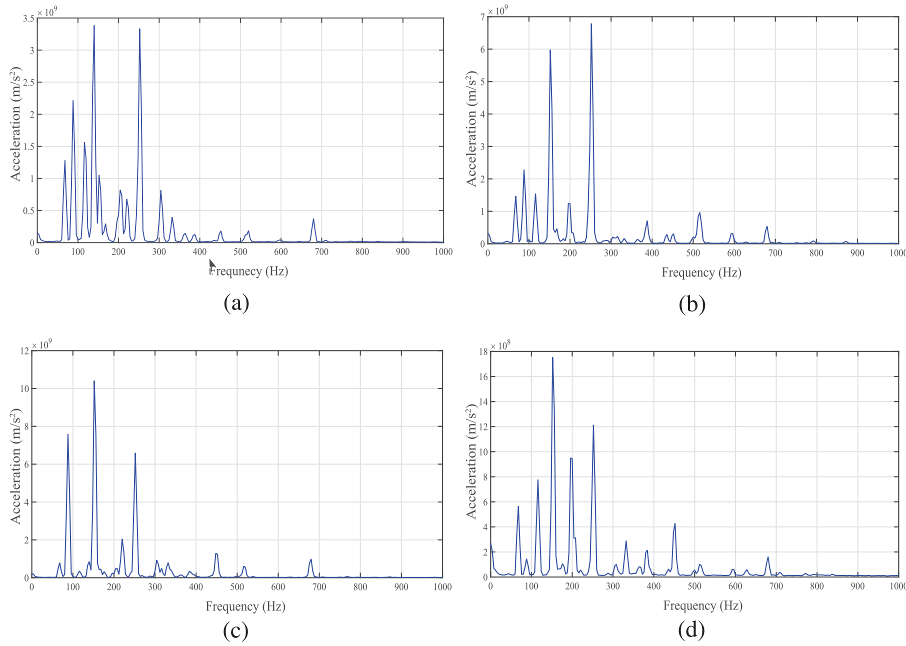

Fig. 4. FFT comparisons of hammer excitation method for different positions of accelerometer: (a) accelerometer at position 1; (b) accelerometer at position 6; (c) accelerometer at position 7; (d) accelerometer at position 8.

Fig. 5. The reverberant chamber.

of the receiving room. Several tests were conducted in which the position of the microphone was modified to estimate the reverberation time. Fig. 8 shows the reverberation time of the reception room for one-twelfth octave frequency bands from 16 Hz to 16 kHz.

3.3. Transmission loss measurement of the thin rectangular plate

In order to validate the analytical expression obtained for transmission loss of a finite thin plate through the SEA theory, a set of experiments were performed in the Sound and Vibration Labora-

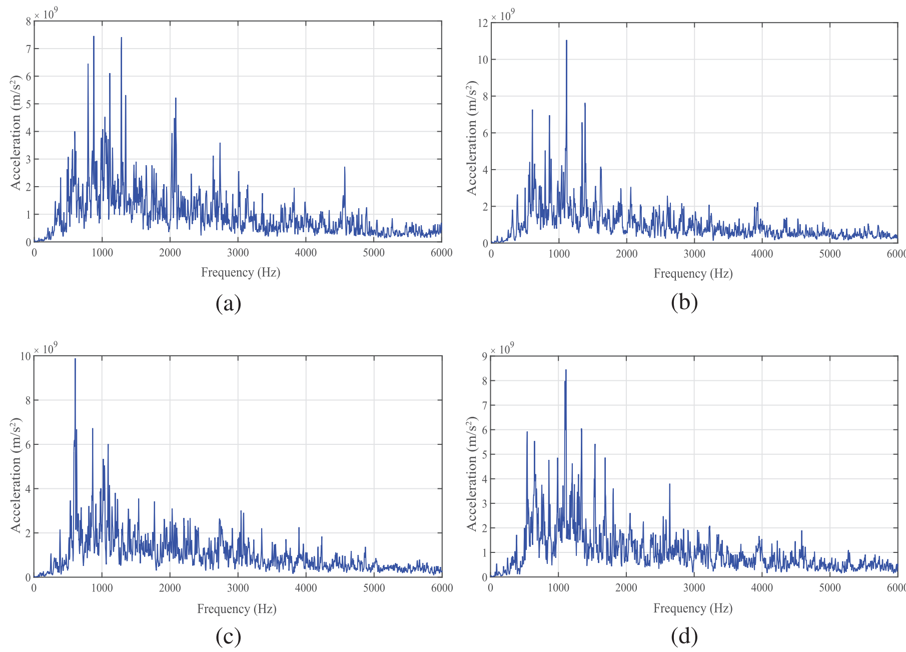

Fig. 6. FFT comparisons of acoustical excitation method for different positions of accelerometer: (a) accelerometer at position 1; (b) accelerometer at position 6; (c) accelerometer at position 7; (d) accelerometer at position 8.

Table 1
Comparison between experimental and theoretical results of first ten natural frequencies of the thin rectangular plate

Mode Number		Natural Frequency (Hz)	
m	n	Experiment	Theory
2	1	140	134
1	1	152	142
3	1	252	238
1	2	304	315
2	2	332	354
4	1	364	372
3	2	384	394
4	2	452	483
5	1	564	544
5	2	648	622

tory of Auburn University. The experiments were made by clamping the steel panel between two cubic reverberation chambers of the same dimensions with sides of length 3.76 m. Fig. 9 shows the reverberation rooms with a window constructed between them where the panel was clamped. The loudspeakers were placed in one of the rooms which was considered as the source room and were connected to the Bruel and Kjaer Pulse system in order to produce a steady random white noise signal. The propagated sound in the source room transmitted through the plate to the receiving room. Since it was needed to provide enough sound power in the source room, three air jet nozzles with different tube dimension were used so that the sound pressure levels in both chambers were at least 10 dB above the background noise. The air jet nozzles are high pressure sources that were utilized to increase the noise level in high frequency bands. The nozzles were connected to the air supply in the source room. The high pressure air flowed through the tubes and interacted with the flow from other tubes to produce high sound pressures in the room. The peak frequency of the noise produced depends on the air flow speed and tube diameter. By arranging flow from tubes to impinge on flow from other tubes in 180° opposite directions, high levels of turbulence and noise is produced. The three air jet nozzles used in the experiment are shown in Fig. 10.

Two experimental methods were used in order to measure the sound transmission loss of the thin rectangular plate. These two approaches are: transmission suite method or two room method and sound intensity method.

3.3.1. Transmission suite method

The transmission suite method which is also known as two rooms method consists of two reverberant chambers, source room and receiving room, which are shown in Fig. 9. The thin rectangular plate under consideration was mounted in the window between two chambers. In order to avoid vibration transmission from the ground to the two rooms and its side effect, the reverberation chambers were mounted on four air bags for each chamber. In order to minimize the background noise in both rooms and also transmission of environmental noise from outside to the rooms, the walls were constructed double-walled with fiberglass in between them. The inner wall which separated the source and receiving rooms was also made in the same way as other walls. Therefore, it can be assumed that the sound transmission between two acoustical spaces only occurred through the plate under test.

The sound transmission loss of the single-walled steel plate can be obtained experimentally by applying the transmission suite method and using the following expression [13]

$$\mathrm{TL} = \mathrm{NR} + 10\log\left[\frac{S_2 c_{\mathrm{air}} T_{60}}{24 V_3 \ln(10)}\right] \tag{46}$$

In order to evaluate the noise reduction, two Bruel and Kjaer microphones (type 4188 L1) with optimized frequency range of $8 - 12500$ Hz were placed in the source and receiving rooms to measure the sound pressure level in each room. The experimental setup is shown in Fig. 11. As explained in the theoretical part, the noise reduction is the difference between sound pressure levels of the source and receiving rooms. The measurements of the sound pressure levels were made several times by changing the position of two microphones in each room. Positions near the plate in the receiving room and near the speakers in the source room include higher sound pressure levels. Therefore, it was important to measure the sound pressure levels at several different positions to

Fig. 7. The experimental setup for measuring the reverberation time of the receiving room.

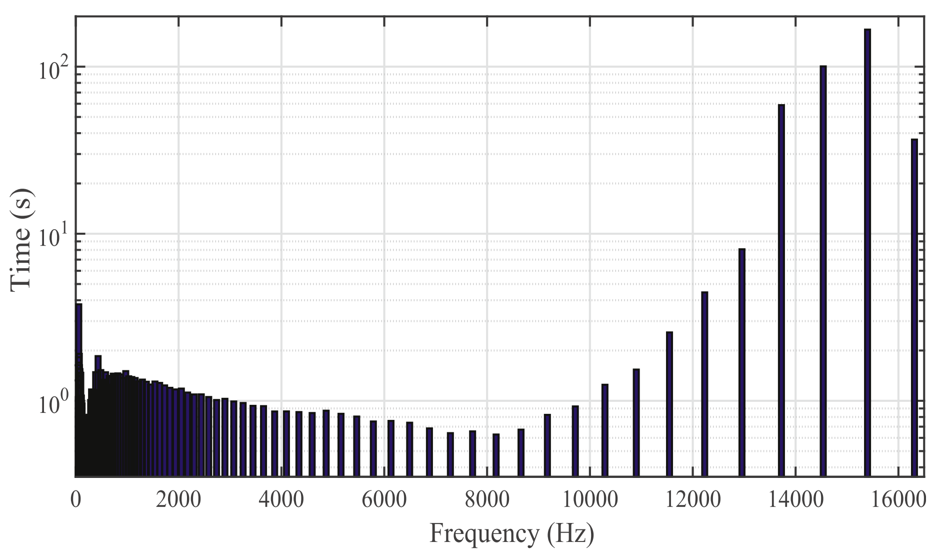

Fig. 8. Reverberation time of the reception room.

obtain a good space-average sound pressure level results in each room. The noise reduction was obtained by calculating the spatial averages of the results. The reverberation time of the receiving room (T_{60}) which was also needed, measured previously and the transmission loss was estimated experimentally using Eq. (46). Fig. 12 shows the sound transmission loss of the thin rectangular plate using the transmission suite method. The speed of sound in air, c_{air}, is considered to be 343 m/s, the surface area of the plate, S_2, and the volume of the reverberation room, V_3, are 0.63 m^2 and 53.16 m^3, respectively.

It is observed that there is a remarkable dip at 10290 Hz. This frequency is the critical frequency of the plate that was predicted by the experiment. The analytical value of the critical frequency can be obtained using Eq. (33) and is 9719 Hz. The percentage of error between the experimental and theoretical results for the critical frequency of the plate is 5.5% which is a good agreement.

3.3.2. *Sound intensity method*

The sound intensity method is based on measuring the sound intensities in the source and reverberation rooms. Then the transmission loss can be obtained using following expression [47]

$$TL = 10\log\left(\frac{I_{incident}}{I_{transmitted}}\right) \tag{47}$$

where $I_{incident}$ and $I_{transmitted}$ are the incident and transmitted intensities, respectively. In order to measure the sound intensity a Bruel and Kjaer intensity probe (type 3599) was used. The probe comprised two 1/2 inch phase-matched microphones (type 4197)

Fig. 9. The source and receiving rooms in the laboratory of sound and vibration.

(a) (b) (c)

Fig. 10. The air jet nozzles: (a) low frequency; (b) medium frequency; (c) high frequency.

(a) (b)

Fig. 11. The experimental setup for the transmission suite method: (a) the source room; (b) the receiving room.

which were positioned face to face and separated by a spacer. The probe contained three spacers: 8.5 mm spacer (type UC-5349), 12 mm spacer (type UC-5269) and 50mm spacer (type UC-5270). Fig. 13 shows the intensity probe with the spacers. The sound intensity measurement in the receiving room was carried out by scanning the entire surface of the plate with the intensity probe following the international standard ISO 15186-1. The scanning procedure repeated several times with all the spacers and the 12 mm spacer revealed the best result in the frequency range of interest.

The sound intensity in the source room cannot be obtained by moving the intensity probe over the plate surface because when

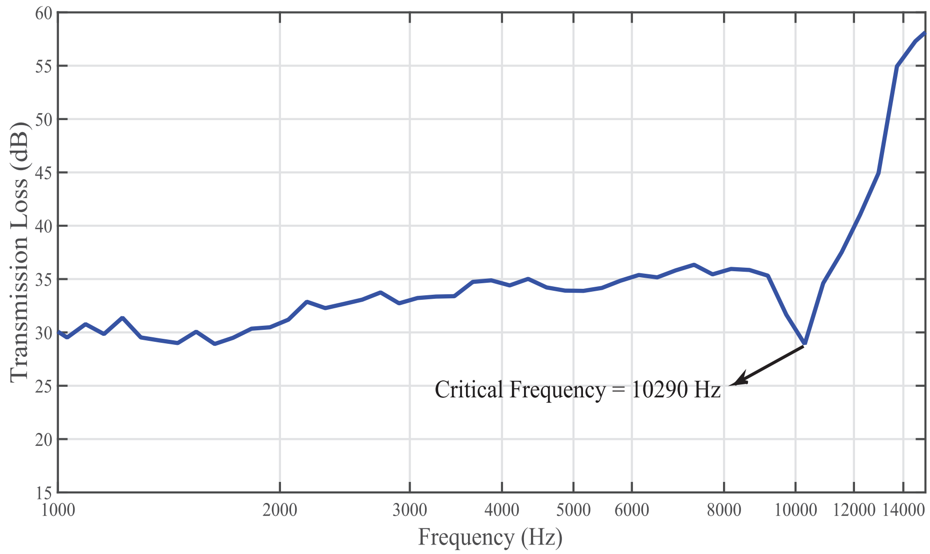

Fig. 12. Sound transmission loss of the thin rectangular plate measured by the transmission suite method.

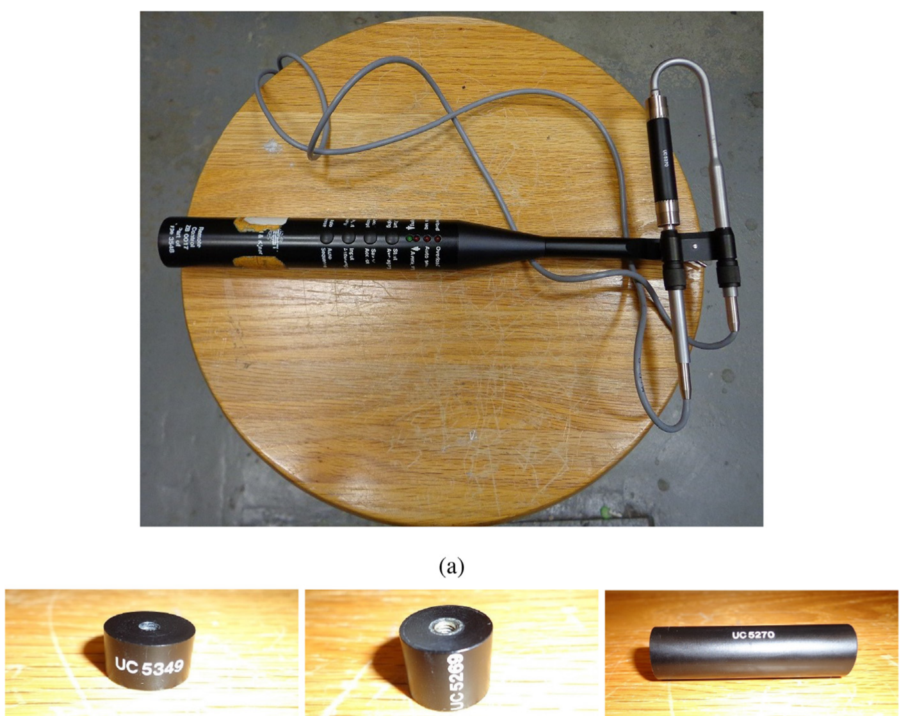

(a)

(b) (c) (d)

Fig. 13. The sound intensity equipments: (a) the sound intensity probe with 50 mm spacer; (b) 8.5 mm spacer (type UC-5349); (c) 12 mm spacer (type UC-5269); (d) 50 mm spacer (type UC-5270).

the noise source is in the same room, the intensity probe measures both the incident and radiated sound waves near the plate and it returns zero result for sound intensity of the source room. Whereas in the receiving room, the intensity probe only measures the transmitted sound. Fig. 14 represents the sound transmission phenomena through the plate between the rooms. Hence, by assuming that the sound field in the source room was diffuse, the incident intensity was evaluated using the measured sound pressure results in the source room which is given by [48]

$$I_{\text{incident}} = \frac{p_{rms}^2}{4\rho_{\text{air}}c_{\text{air}}} \tag{48}$$

where p_{rms} is the measured average sound pressure in the source room.

The sound intensity of the source room was also measured directly without considering the assumption of diffuse sound field in the source room. In this approach, the plate was removed and the sound intensity was measured by scanning the empty space

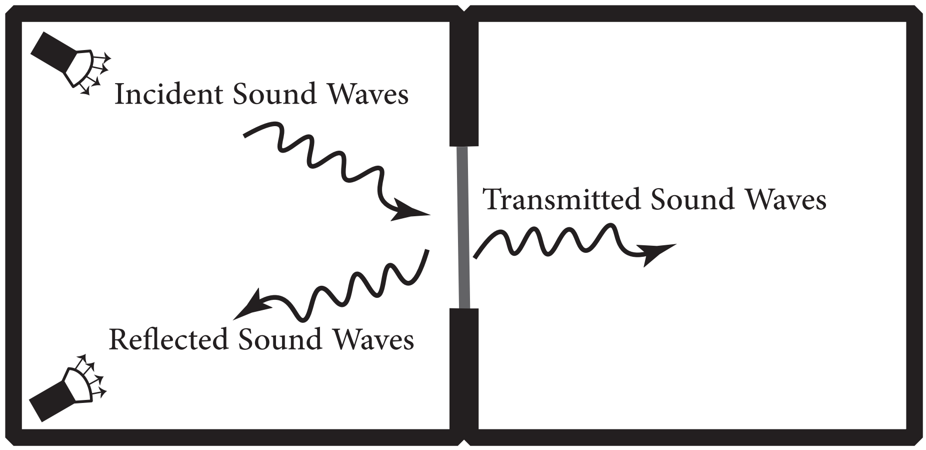

Fig. 14. Schematic illustration of sound transmission through a plate.

that was belonged to the plate. The measurements were carried out from the receiving side of the window Thus, the sound intensity probe was subjected to the incident sound waves. Hence, the incident intensity was achieved directly. It should be mentioned that since the loudspeakers are working while measuring the incident intensity, precautions should be taken to avoid hearing damage caused by exposure to loud noise.

The transmission losses obtained by the sound intensity method which is also known as the two-microphones method due to the two closely spaced microphones used in the probe, using both direct and indirect approaches for measuring incident acoustic intensity are shown in Fig. 15. It is seen that the procedure which was performed to obtain the incident sound intensity inside the room affected the transmission loss trend. The direct approach predicted the critical frequency of the thin rectangular plate at 9669 Hz (0.5% error) whereas the critical frequency estimated by the indirect approach is 10480 Hz (7.8% error). Not only the value of critical frequency is different in these two approaches but also the predicted transmission loss has about 20 dB difference. The critical frequency plays a significant role in specifying the acoustic behavior of plates, because at this particular frequency plates become acoustically transparent which means that noise transmission occurs easily between source and receiving rooms. Therefore, it is of great importance to use a method that has higher accuracy. In the following section, the experimental results of transmission loss are compared with the analytical ones.

3.3.3. Comparison of analytical and experimental results

A comparison is made between the experimental measurements of the sound transmission loss of the thin single-walled rectangular plate and analytical calculations based on SEA theory and is represented in Fig. 16. Since the angle of incidence for the incident sound wave is not obvious, the diffuse and random incidence is considered in computing the coupling loss factor between source and receiving rooms. The internal loss factor of the plate is considered to be $\eta_2 = 0.02$ according to the setup condition and the density of air is considered to be $\rho_{air} = 1.21\ \mathrm{kg/m^3}$. It can be seen from Fig. 16 that the analytical result and the transmission loss measured using sound intensity method with direct approach are in very good agreement specifically at critical frequency. The transmission suite method and the sound intensity method with indirect approach followed a similar trend and showed some discrepancies in comparison with the analytical calculations in the

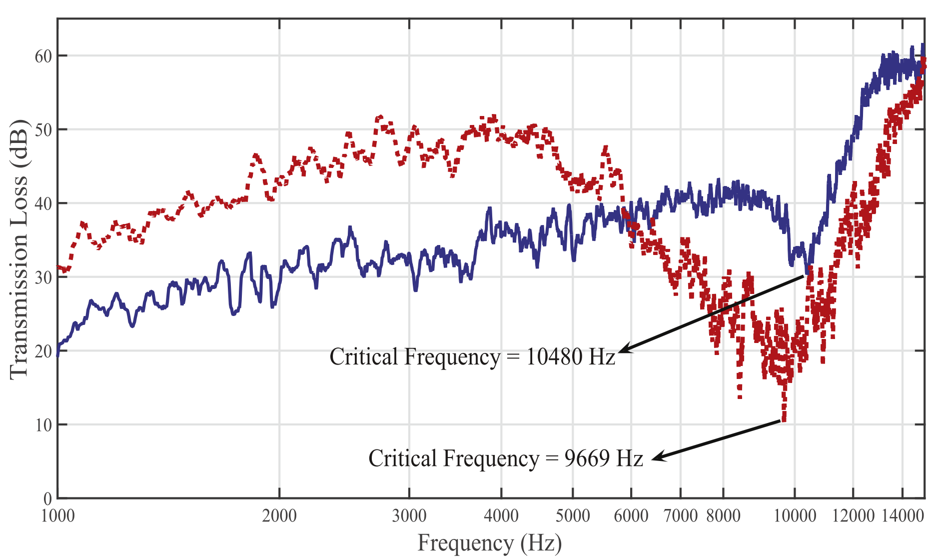

Fig. 15. Sound transmission loss of the rectangular plate measured by the sound intensity method; Incident intensity obtained indirectly using sound pressure results (———), Incident intensity measured directly (- - - - -).

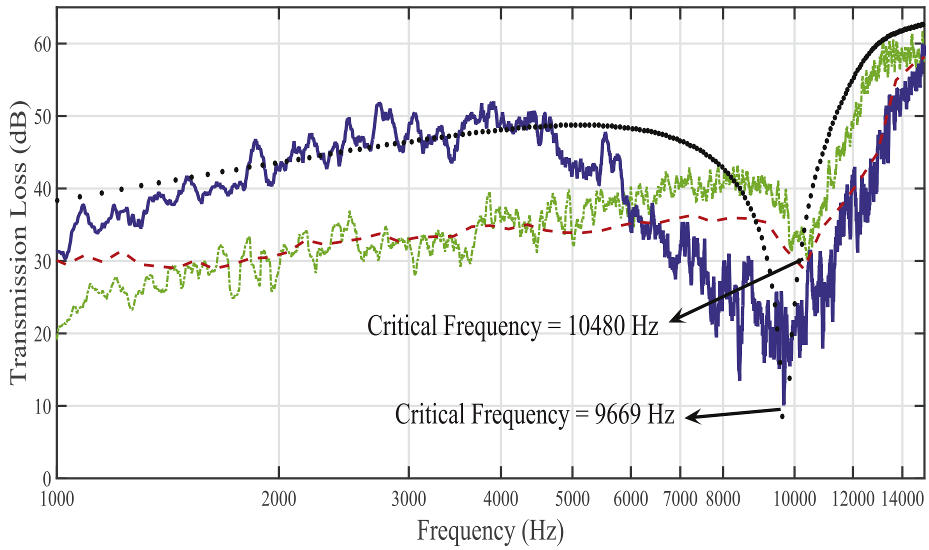

Fig. 16. Comparison between experimental and analytical results for sound transmission loss of the thin single-walled rectangular plate; SEA theory (········), Transmission suite method (------), Sound intensity method with direct approach (——) and Sound intensity method with indirect approach (-·-·-·-).

low and medium frequency bands and at the critical frequency. As mentioned before, the sound transmission loss prediction at the critical frequency has a high priority in evaluating the sound insulation performance of a structure made of plate elements. As it can be observed in Fig. 16, the analytical SEA-based model predicted the critical frequency to be 9669 Hz which is very close to the result obtained by Eq. (33) which is 9719 Hz. The sound intensity method using the direct approach also predicted the critical frequency of the plate and its sound transmission loss to be similar to the analytical model prediction. Therefore, the sound intensity method using the direct approach, which is explained in the previous section, is an appropriate experimental technique for the analysis of the sound transmission loss of a plate structure due to its high accuracy.

4. Parametric studies

The analytical model is also developed for double-walled plates in the theoretical section and can be used for a proper and efficient design of vibro-acoustic systems that include plate structures. In order to examine the efficacy of different parameters on improving acoustic performance of double-walled structures, parametric studies are conducted.

As mentioned in the introduction, various techniques have been proposed to reduce noise transmission through a plate shape structure. Using absorbing materials such as fiberglass on each side of the plate or in the cavity between two walls of the plate is a proper way to increase sound transmission loss without any significant influence on the weight of the structure and its natural frequencies. Therefore, using absorbing material is studied analytically and experimentally here as a main approach to improve acoustic performance of plates.

4.1. Effect of single- and double-walled constructions

Fig. 17 shows the sound transmission losses of single- and double-walled thin rectangular plates. The dimensions and material properties are similar to the plate used in the experiment. The cavity depth in the double-walled plate is $d = 0.01$ m. It can be seen that the double-walled configuration provided a better performance of sound transmission loss than single-walled plate. Its effect at the critical frequency of the panel and the frequency region near the critical frequency was quite noticeable. The double-walled configuration with a cavity contained only air and the cavity loss factor of $\eta_3 = 0.01$ caused about 30 dB increase in the transmission loss of the panel at these frequencies.

4.2. Effect of absorbing materials on sound transmission loss of single-walled plates

Absorbing material such as fiberglass can be used on the source or receiving side of the plate or inside the cavity for the double-walled plate. Fig. 18 shows the transmission losses obtained experimentally using sound intensity method with direct approach for the cases of applying absorbing material as a sound insulation on each side of the single-walled plate. It is seen that applying absorbing material did not have much effect on the transmission loss of a single-walled plate. Using absorbing material on the source and receiving sides of the plate caused about 10 dB and 5 dB enhancement, respectively in low and medium frequency regions. However, their effects in high frequency region and at the critical frequency was not noticeable.

4.3. Effect of absorbing material on sound transmission loss of double-walled plates

It is seen in Fig. 17 that making a double-walled panel with cavity depth of 1 cm improves the transmission loss in all frequency ranges and specifically about 30 dB at the critical frequency of the panel. With this information, the authors suggest filling the cavity with lightweight absorbing materials such as fiberglass to achieve more noise reduction. In order to examine the performance of absorbing materials in double-walled plates, it is necessary to find the absorption coefficient of the absorbing material under investigation. Therefore, several reverberation time measurements were performed in one of the reverberation chambers in which the floor was covered with the fiberglass. By measuring the reverberation time and using the Sabine's equation [49]

$$T_{60} = \frac{0.16V}{\sum_{i=1}^{6} S_i \alpha_i} \tag{49}$$

in which V is the volume of the reverberation chamber, i is the number of room surface, S is the area of each room surface and α is the

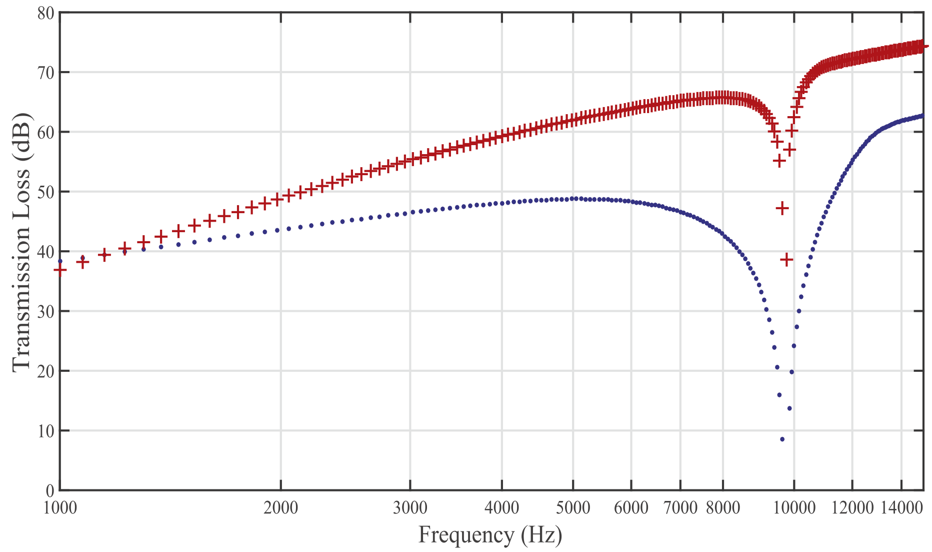

Fig. 17. The effects of single (⋯⋯) and double (+++++) walled thin rectangular plates on transmission losses.

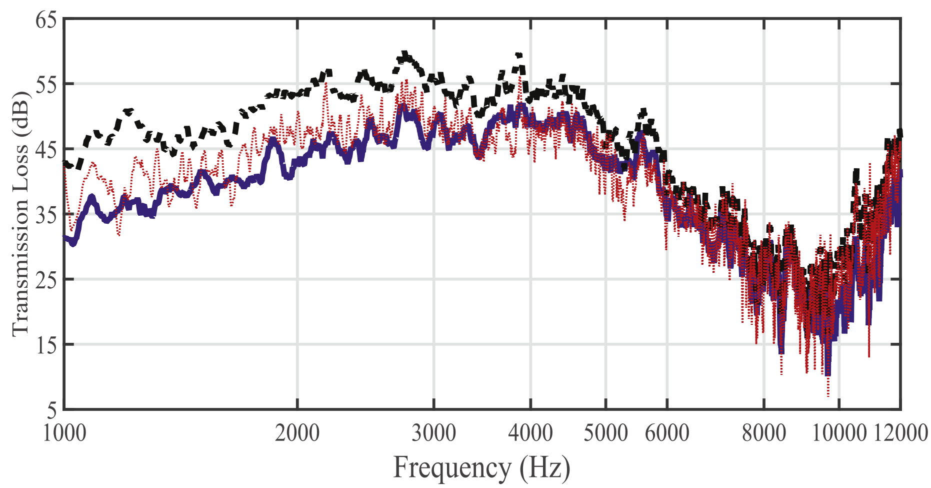

Fig. 18. The effects of using absorbing material for a single-walled plate: Absorbing material on the source side (⋯⋯); Absorbing material on the receiving side (⋯⋯) and Single-walled plate without absorbing material (——).

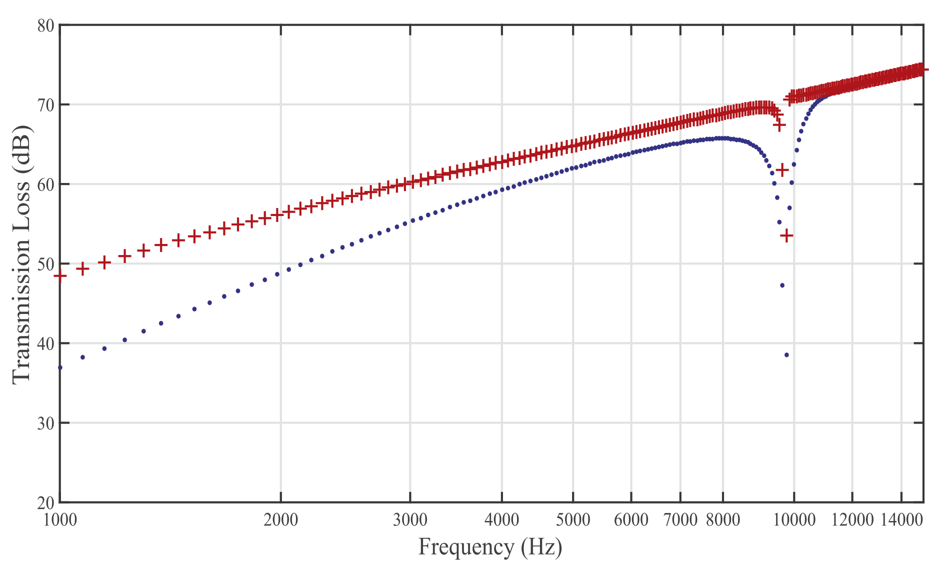

Fig. 19. Comparison of the sound transmission loss of the double-walled plate with (+++++) and without (⋯⋯) fiberglass inside the cavity.

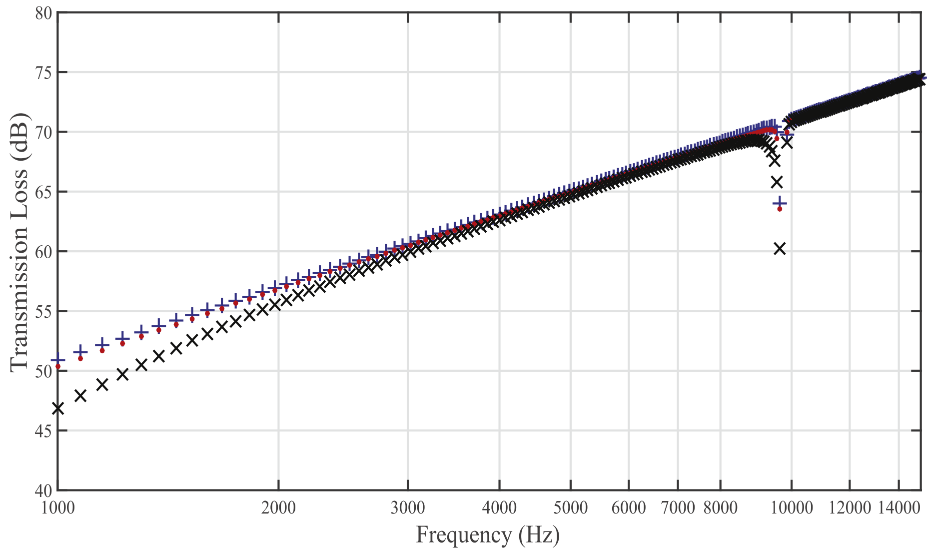

Fig. 20. Effect of cavity depth on noise reduction of a double-walled plate with absorbing material; $d = 0.5$ cm ($\times\times\times\times$); $d = 5$ cm (·········) and $d = 20$ cm (+++++).

absorption coefficient of each room surface, the absorbing coefficient of the fiberglass was obtained $\alpha = 0.32$. Hence, the internal loss factor of the cavity contained fiberglass in the double-walled SEA model is assumed as $\eta_3 = 0.32$.

Fig. 19 shows the sound transmission loss of the double-walled plate with fiberglass inside the cavity compared with the case without fiberglass. It is seen that filling the cavity with fiberglass has a positive effect on noise reduction and the transmission loss is improved about 15 dB at the critical frequency which is a good progress in decreasing noise transmission through double-walled plate structures. Besides fiberglass influence on sound transmission at the critical frequency, it is also effective in low and medium frequency regions.

4.4. Effect of cavity depth on sound transmission loss of double-walled plates

It was found out in Fig. 19 that using absorbing material is an appropriate way to reach an improvement in sound insulation performance of double-walled plate structures. It is of great significance to understand the effectiveness of cavity depth while it is filled with absorbing materials. Therefore, a comparison is made for three cavity depths of 0.5 cm, 5 cm and 20 cm. The comparison is shown in Fig. 20. It can be seen that increasing the cavity depth from 0.5 cm to 20 cm does not make any significant change in the sound transmission loss trend. Its only effect is an enhancement of slightly less than 5dB in low frequency region and at the critical frequency. Hence, it is deduced that increasing the depth of the cavity in double-walled plates which may cause some problems in designing the structure is not very helpful in noise reduction.

5. Conclusions

In this paper, the statistical energy analysis (SEA) approach was used in order to study the sound transmission through a thin single-walled rectangular plate and it was developed for a thin double-walled rectangular plate. The effects of structural and cavity damping were considered in the derivation and the parameters that are involved in SEA modeling such as modal density, loss factors and radiation efficiency were obtained for both single- and double-walled plates. Then two expressions were presented for the transmission loss of single- and double-walled plate structures. An experimental setup was also conducted in order to predict the transmission loss experimentally. First, natural frequencies of a single-walled plate were evaluated using two methods of hammer and acoustical excitations and compared with the analytical results which showed a good agreement. It was observed that the contact method in which a modal hammer was utilized is applicable in low frequency region and the non-contact method in which a loudspeaker was used for the acoustical excitation is more effective in medium and high frequency regions.

Then the sound transmission loss was measured and the results compared with the analytical ones. Three experimental methods were used in order to predict the sound transmission loss: Transmission suite method, sound intensity method with direct approach and sound intensity method with indirect approach. The transmission suite method and sound intensity method are based on measuring the sound pressure levels and acoustic intensities in both source and receiving rooms, respectively. The incident sound intensity in the indirect approach were calculated by using the measured sound pressure level in the source room, whereas it was measured directly in the direct approach. It was shown that the sound intensity method with direct approach gave the most accurate result with an error of 0.5% for the transmission loss at the critical frequency.

The effects of using absorbing material in single- and double-walled plate constructions were examined. Theoretical analysis shows that a double-walled panel results in more noise reduction in all frequency regions compared with a single-walled panel and specifically it improves the noise reduction by about 30 dB at the critical frequency. It was shown theoretically that filling the cavity of a double-walled plate with absorbing material is a suitable way to achieve high sound insulation performance.

Acknowledgments

The authors would like to thank the Department of Mechanical Engineering of Auburn University for providing the facilities during the experimental research in the Sound and Vibration Laboratory of Wilmore Laboratories. M. Maksotskaya, the special assistant at International Institute of Acoustics and Vibration and F. Taha, master's student at Sound and Vibration Laboratory of Auburn University are also acknowledged for the help during the research.

Appendix A

The procedure to obtain the mode shape of vibration for a thin rectangular clamped plate is explained as follows:

Since free vibrations are assumed, the motion is considered to be harmonic.

$$w(x,y,t) = W(x,y)\sin(\omega_{mn}t), \tag{A-1}$$

where W is a function of position coordinates. By substituting Eq. (A-1) into Eq. (1), the differential equation governing the free vibration of the plate can be obtained as

$$D\left(\frac{\partial^4 W}{\partial x^4} + 2\frac{\partial^4 W}{\partial x^2 \partial y^2} + \frac{\partial^4 W}{\partial y^4}\right) - \rho h \omega_{mn}^2 W = 0. \tag{A-2}$$

By using the Rayleigh-Ritz method, the transverse displacement of plate $W(x,y)$ can be written as

$$W(x,y) = \sum_{m=1}^{\infty}\sum_{n=1}^{\infty} X_m(x) Y_n(y), \tag{A-3}$$

in which $X_m(x)$ and $Y_n(y)$ denote the shape functions describing the modes of vibration along the x and y directions, respectively. The assumed shape functions must satisfy the boundary conditions of the plate. In this paper the clamped and immovable boundary conditions at all of the edges of the rectangular plate are considered, which are expressed as

$$W(x,y) = \frac{\partial W(x,y)}{\partial x} = 0 \text{ at } x = 0 \text{ and } l_x, \tag{A-4a}$$

and

$$W(x,y) = \frac{\partial W(x,y)}{\partial y} = 0 \text{ at } y = 0 \text{ and } l_y. \tag{A-4b}$$

By using beam characteristic functions having the boundary conditions of the plate, the following shape functions are obtained [33]

$$X_m(x) = \left[\cosh\left(\frac{k_m x}{l_x}\right) - \cos\left(\frac{k_m x}{l_x}\right)\right] - \frac{\cosh(k_m) - \cos(k_m)}{\sinh(k_m) - \sin(k_m)}\left[\sinh\left(\frac{k_m x}{l_x}\right) - \sin\left(\frac{k_m x}{l_x}\right)\right], \tag{A-5a}$$

$$Y_n(y) = \left[\cosh\left(\frac{k_n y}{l_y}\right) - \cos\left(\frac{k_n y}{l_y}\right)\right] - \frac{\cosh(k_n) - \cos(k_n)}{\sinh(k_n) - \sin(k_n)}\left[\sinh\left(\frac{k_n y}{l_y}\right) - \sin\left(\frac{k_n y}{l_y}\right)\right]. \tag{A-5b}$$

where the values of k_m and k_n are calculated as roots of Eqs. (A-6a) and (A-6b), respectively.

$$\cosh(k_m)\cos(k_m) - 1 = 0, \tag{A-6a}$$

$$\cosh(k_n)\cos(k_n) - 1 = 0. \tag{A-6b}$$

References

[1] Crocker MJ. Handbook of noise and vibration control. John Wiley & Sons; 2007.
[2] Tristán-Hernández E, Garća IP, Navarro JML, Campos-Cantón I, Kolosovas-Machuca ES. Evaluation of psychoacoustic annoyance and perception of noise annoyance inside university facilities. Int J Acoust Vib 2018;23:3–8.
[3] Trochidis A, Kalaroutis A. Sound transmission through double partitions with cavity absorption. J Sound Vib 1986;107:321–7.
[4] Chonan S, Kugo Y. Acoustic characteristics and the design of two-layered soundproof plates. J Sound Vib 1989;129:501–11.
[5] Steel JA. Sound transmission between plates in framed structures. J Sound Vib 1994;178:379–94.
[6] Osipov A, Mees P, Vermeir G. Low-frequency airborne sound transmission through single partitions in buildings. Appl Acoust 1997;52:273–88.
[7] Liu GR, Cai C, Lam KY. Sound reflection and transmission of compliant plate-like structures by a plane sound wave excitation. J Sound Vib 2000;230:809–24.
[8] Campolina B, Dauchez N, Atalla N, Doutres O. Effect of porous material compression on the sound transmission of a covered single leaf panel. Appl Acoust 2012;73:791–7.
[9] Zhou J, Bhaskar A, Zhang X. Optimization for sound transmission through a double-wall panel. Appl Acoust 2013;74:1422–8.
[10] Pellicier A, Trompette N. A review of analytical methods, based on the wave approach, to compute partitions transmission loss. Appl Acoust 2007;68:1192–212.
[11] Maidanik G. Response of ribbed panels to reverberant acoustic fields. J Acoust Soc Am 1962;34:809–26.
[12] Lyon RH. Statistical energy analysis of dynamical systems: theory and applications; 1975.
[13] Crocker MJ, Price AJ. Sound transmission using statistical energy analysis. J Sound Vib 1969;9:469–86.
[14] Jean P, Roland J. Simplified sea-type models to predict the sound insulation between dwellings. Appl Acoust 1993;40:201–11.
[15] Hynna P, Klinge P, Vuoksinen J. Prediction of structure-borne sound transmission in large welded ship structures using statistical energy analysis. J Sound Vib 1995;180:583–607.
[16] Craik RJM, Steel JA, Evans DI. Statistical energy analysis of structure-borne sound transmission at low frequencies. J Sound Vib 1991;144:95–107.
[17] Osipov A, Vermeir G. Sound transmission in buildings with elastic layers at joints. Appl Acoust 1996;49:141–62.
[18] Hopkins C. Sound transmission across a separating and flanking cavity wall construction. Appl Acoust 1997;52:259–72.
[19] Craik RJM, Smith RS. Sound transmission through double leaf lightweight partitions Part I: airborne sound. Appl Acoust 2000;61:223–45.
[20] Craik RJM, Smith RS. Sound transmission through lightweight parallel plates. Part II: structure-borne sound. Appl Acoust 2000;61:247–69.
[21] Zhou R, Crocker MJ. Sound transmission loss of foam-filled honeycomb sandwich panels using statistical energy analysis and theoretical and measured dynamic properties. J Sound Vib 2010;329:673–86.
[22] Reynders E, Langley RS, Dijckmans A, Vermeir G. A hybrid finite element-statistical energy analysis approach to robust sound transmission modeling. J Sound Vib 2014;333:4621–36.
[23] Mondal S, Chakraborty S. Estimation of viscous damping parameters of fibre reinforced plastic plates using finite element model updating. Int J Acoust Vib 2018;23:26–34.
[24] Mishra AK, Mohammed A, Chakraborty S. Improved numerical modelling of fiber reinforced plastics i-beam from experimental modal testing and finite element model updating. Int J Acoust Vib 2018;23:16–25.
[25] Vigran TE. Sound transmission in multilayered structures-introducing finite structural connections in the transfer matrix method. Appl Acoust 2010;71:39–44.
[26] Jung J, Kook J, Goo S, Wang S. Sound transmission analysis of plate structures using the finite element method and elementary radiator approach with radiator error index. Adv Eng Softw 2017;112:1–15.
[27] Wang YS, Crocker MJ, Raju PK. Theoretical and experimental evaluation of transmission loss of cylinders. J Am Inst Aeronaut Astronaut 1983;21:186–92.
[28] Chen YH, Chen KT, Chaing YH. Plate-damping measurements in a single reverberation room. Appl Acoust 1996;47:251–61.
[29] Connelly M, Hodgson M. Experimental investigation of the sound transmission of vegetated roofs. Appl Acoust 2013;74:1136–43.
[30] Oliazadeh P, Farshidianfar A, Crocker MJ. Experimental and analytical investigation on sound transmission loss of cylindrical shells with absorbing material. J Sound Vib 2018;434:28–43.
[31] Li H, Luo H, Sun W, Wen B. The influence of elastic boundary on modal parameters of thin cylindrical shell. Int J Acoust Vib 2018;23:93–105.
[32] Florence SJK, Renji K, Subramanian K. Modal density of honeycomb sandwich composite cylindrical shells considering transverse shear deformation. Int J Acoust Vib 2018;23:83–92.
[33] Leissa AW. Vibration of plates, Technical Report, Ohio State Univ Columbus; 1969.
[34] Price AJ, Crocker MJ. Sound transmission through double panels using statistical energy analysis. J Acoust Soc Am 1970;47:683–93.
[35] Fahy FJ, Gardonio P. Sound and structural vibration: radiation, transmission and response. Academic Press; 2007.
[36] Rindel JH. Dispersion and absorption of structure-borne sound in acoustically thick plates. Appl Acoust 1994;41:97–111.
[37] Marsch J, Pörschmann C. Frequency dependent control of reverberation time for auditory virtual environments. Appl Acoust 2000;61:189–98.
[38] Churchill C, Hopkins C. Prediction of airborne sound transmission across a timber–concrete composite floor using statistical energy analysis. Appl Acoust 2016;110:145–59.
[39] Liu B, Jiang Y, Chang D. Sound transmission of a spherical sound wave through a finite plate. J Sound Vib 2017;410:209–16.
[40] Yairi M, Koga T, Takebayashi K, Sakagami K. Transmission of a spherical sound wave through a single-leaf wall: mass law for spherical wave incidence. Appl Acoust 2014;75:67–71.
[41] Craik RJM. Non-resonant sound transmission through double walls using statistical energy analysis. Appl Acoust 2003;64:325–41.
[42] Craik RJM, Wilson R. Sound transmission through parallel plates coupled along a line. Appl Acoust 1996;49:353–72.

[43] Arcas K, Chaigne A. On the quality of plate reverberation. Appl Acoust 2010;71:147–56.
[44] Oppenheimer CH, Dubowsky S. A radiation efficiency for unbaffled plates with experimental validation. J Sound Vib 1997;199:473–89.
[45] Putra A, Thompson DJ. Sound radiation from rectangular baffled and unbaffled plates. Appl Acoust 2010;71:1113–25.
[46] Lai JCS, Qi D. Sound transmission loss measurements using the sound intensity technique Part 1: The effects of reverberation time. Appl Acoust 1993;40:311–24.
[47] Halliwell RE, Warnock ACC. Sound transmission loss: comparison of conventional techniques with sound intensity techniques. J Acoust Soc Am 1985;77:2094–103.
[48] Crocker MJ, Raju PK, Forssen B. Measurement of transmission loss of panels by the direct determination of transmitted acoustic intensity. Noise Control Eng 1981;17:6–11.
[49] Fothergill LC. An investigation of simple methods for assessing reverberation time. Appl Acoust 1982;15:11–29.